



# Orientation dependence of structural, electrical and magnetic properties of $\text{La}_{0.9}\text{Sr}_{0.1}\text{MnO}_3$ thin films



Lu Yin, Chuanbin Wang<sup>\*</sup>, Qiang Shen, Lianmeng Zhang

State Key Lab of Advanced Technology for Materials Synthesis and Processing, Wuhan University of Technology, Wuhan, 430070, China

## ARTICLE INFO

### Article history:

Received 3 September 2016

Received in revised form

18 October 2016

Accepted 20 October 2016

Available online 21 October 2016

### Keywords:

$\text{La}_{0.9}\text{Sr}_{0.1}\text{MnO}_3$  thin films

Film orientation

Electrical transport properties

Magnetoresistance

## ABSTRACT

In this paper,  $\text{La}_{0.9}\text{Sr}_{0.1}\text{MnO}_3$  thin films were grown epitaxially on (100), (110), and (111)  $\text{LaAlO}_3$  substrates, and the effects of film orientation on the structural, electrical and magnetic properties were investigated. Compared with the corresponding bulk material, all the films show metal-insulator transition around room temperature with a significantly enhanced Curie temperature. The in-plane compressive strain, coercivity, resistivity and magnetoresistance (MR) of the films increase in the order (100) < (110) < (111). While the paramagnetic-ferromagnetic transition temperature ( $T_C$ ) and metal-insulator transition temperature ( $T_{MI}$ ) of the films increase in the order (111) < (110) < (100). These results demonstrate that the lattice distortion of  $\text{MnO}_6$  octahedron can be tuned by controlling the film orientation, which can be an effective route to adjust the structural, electrical and magnetic properties of  $\text{La}_{0.9}\text{Sr}_{0.1}\text{MnO}_3$  films.

© 2016 Elsevier B.V. All rights reserved.

## 1. Introduction

Doped perovskite manganites  $\text{La}_{1-x}\text{B}_x\text{MnO}_3$  (L is a trivalent rare-earth ion and B is a divalent alkali-earth ion) have attracted widespread attention due to their distinctive magnetic and electronic behaviors such as colossal magnetoresistance (CMR) [1], phase separation (PS) [2], and spin/charge/orbital ordering (SO/CO/OO) [3–5], which can be attributed to a complex interplay among ferromagnetic double-exchange interaction [6], antiferromagnetic super-exchange interaction [7], Jahn-Teller distortion [8], and charge-orbital ordering interactions. This makes them promising for applications in magnetic random access memories, magnetic sensors, and various spintronic devices [9].

Depending on the doping level  $x$ , the compound  $\text{La}_{1-x}\text{Sr}_x\text{MnO}_3$  exhibits various electronic, magnetic, and structural phase transitions at different temperatures [10,11]. Lightly doped  $\text{La}_{1-x}\text{Sr}_x\text{MnO}_3$  ( $x < 0.15$ ) has shown a great variety of intriguing phenomena and thus is being of great interest. Urushibara et al. [10] have found that the largest magnetoresistance effect was observed for samples with  $x \leq 0.175$ . For those with higher Sr doping levels, the magnetoresistance dropped significantly. A similar result has been reported in  $\text{La}_{0.9}\text{Sr}_{0.1}\text{MnO}_3$  films by Chen et al. [12]. Additionally, they have

observed that the transition temperature from ferromagnetic metallic to paramagnetic insulating phases for  $\text{La}_{0.9}\text{Sr}_{0.1}\text{MnO}_3$  films could reach as high as 308 K, which is nearly double the value of 145 K observed in bulk compounds [10]. And the epitaxial strain induced by the film/substrate lattice mismatch is considered to be responsible for the significant enhancement in Curie temperature ( $T_C$ ). According to theoretical calculations, the strain could induce different patterns of octahedral distortions by oxygen octahedral rotations and their coupling to Jahn-Teller distortions which lead to crystal field splitting of ( $d_{x^2-y^2}^2/d_{3z^2-r^2}^2$ ) orbitals, thus modifying their electron occupancy and resulting in complex orbital reconstruction [13,14]. It is clear that the physical properties of the films depend strongly on their strain states. In addition to the lattice mismatch, the film orientation can also determine the strain states, and thus dramatically affect the growth [15], magnetic anisotropy [16], and transport properties [17]. However, nearly all of the studies related to the effect of orientation have focused on  $\text{La}_{1-x}\text{Sr}_x\text{MnO}_3$  with a doping level of  $x \sim 0.3$  which has the highest Curie temperature. Very little attention has been paid to the orientation effects in lightly doped  $\text{La}_{1-x}\text{Sr}_x\text{MnO}_3$  ( $x < 0.15$ ). Moreover, previous studies have demonstrated that the strain could induce a different Curie temperature variation in  $\text{La}_{1-x}\text{Sr}_x\text{MnO}_3$  films with different doping level. For example, the fully strained  $\text{La}_{0.7}\text{Sr}_{0.3}\text{MnO}_3$  films generally show a lower  $T_C$  as compared to the bulk [17,18], while the case for  $\text{La}_{0.9}\text{Sr}_{0.1}\text{MnO}_3$  films is the reverse [12,19]. As such, the orientation effects in lightly doped  $\text{La}_{1-x}\text{Sr}_x\text{MnO}_3$  films are unpredictable and

<sup>\*</sup> Corresponding author.

E-mail address: [ilab@whut.edu.cn](mailto:ilab@whut.edu.cn) (C. Wang).

deserve further research.

In this study,  $\text{La}_{0.9}\text{Sr}_{0.1}\text{MnO}_3$  thin films were epitaxially grown on (100), (110), and (111)  $\text{LaAlO}_3$  single crystal substrates using magnetron sputtering. The effects of thin film orientation on the microstructural, magnetic and transport properties were investigated systematically.

## 2. Experimental details

The  $\text{La}_{0.9}\text{Sr}_{0.1}\text{MnO}_3$  (LSMO) films with thickness of 70 nm were grown on (100), (110) and (111)  $\text{LaAlO}_3$  (LAO, cubic,  $a = 3.793 \text{ \AA}$ ) single crystal substrate using DC-magnetron sputtering under the same conditions. The substrate temperature was kept at room temperature and the gas pressure of deposition was fixed at 1 Pa with an  $\text{Ar}/\text{O}_2$  ratio of 1:1. After deposition, each film was annealed in air at  $800^\circ\text{C}$  for 1 h for achieving perovskite structure. The structure and epitaxy of the films were characterized by X-ray diffraction (XRD, Rigaku Ultima III)  $\theta$ - $2\theta$ , and  $\phi$ -scan measurements using the Schulz reflection method. The thickness of the films was examined by field emission scanning electron microscopy (FESEM, FEI Quanta FEG250). The magnetic properties of the films were measured using a superconducting quantum interference device (SQUID, Quantum Design) magnetometer. The diamagnetic contribution of the substrate was subtracted from the data. During the magnetic measurements, the field was applied in parallel to the film plane to minimize the demagnetization effects. Resistivity and magnetoresistance were measured by a physical property measurement system (PPMS, Quantum Design) using standard four-point method.

## 3. Results and discussion

### 3.1. Structural analysis

Fig. 1 (a) shows the  $\theta$ - $2\theta$  scan of XRD taken from a series of the LSMO films grown on (100)-, (110)-, and (111)-oriented LAO

substrates, respectively. It indicates that each film is single crystal with the similar orientation to the substrate. The out-of-plane lattice parameters calculated from the  $\theta$ - $2\theta$  scan are 3.873, 3.883, 3.889  $\text{\AA}$  for LSMO (100), LSMO (110), LSMO (111), respectively. These values are larger than the  $c$ -axis lattice parameter ( $c \sim 3.868 \text{ \AA}$ ) [12] of the LSMO bulk material, indicating that these films are subjected to an out-of-plane tensile and in-plane compressive strain, which is consistent with the fact that the lattice parameters of the LSMO bulk material are larger than those of the LAO substrate. The out-of-plane tensile strain is defined as  $\epsilon_{zz} = (c_{\text{film}} - c_{\text{bulk}})/c_{\text{bulk}}$  and the in-plane compressive strain can be obtained through the Poisson relation  $\epsilon_{xx} = -(1-\nu)\epsilon_{zz}/2\nu$  with  $\nu = 0.4$  [20], which is calculated to be  $-0.1\%$ ,  $-0.29\%$ , and  $-0.41\%$  for LSMO (100), LSMO (110), LSMO (111) films, respectively.

The in-plane textures of the LSMO films were measured by X-ray  $\phi$ -scans, as shown in Fig. 1(b)–(d). For the LSMO films grown on the (100)- and (111)-oriented LAO substrates in Fig. 1(d) and (b), the (110) reflection of both LSMO and LAO show clearly a set of four symmetric peaks and three symmetric peaks respectively with  $90^\circ$  and  $120^\circ$  interval, indicating the LSMO films on the LAO (100) and (111) substrates present an epitaxial relationship of (100)[110] LSMO//[(100)[110] LAO and (111)[110] LSMO//[(111)[110] LAO, respectively. While for the (110)-oriented film, the (100) plane is selected to determine the epitaxial relationship. As shown in Fig. 1(c), two symmetric peaks with  $180^\circ$  interval is observed in the LSMO (110) film, suggesting the epitaxial relationship as (110)[100] LSMO//[(110)[100] LAO.

### 3.2. Magnetic properties

The temperature dependent magnetization under a magnetic field of 500 Oe is shown in Fig. 2(a). With decreasing temperature, all the LSMO thin films exhibit a paramagnetic to ferromagnetic (PM-FM) transition at the Curie temperature which is defined as the one corresponding to the peak of  $\text{dM}/\text{dT}$ . It is observed that the  $T_C$  are 284 K, 269 K and 263 K respectively for (100)-, (110)-, and

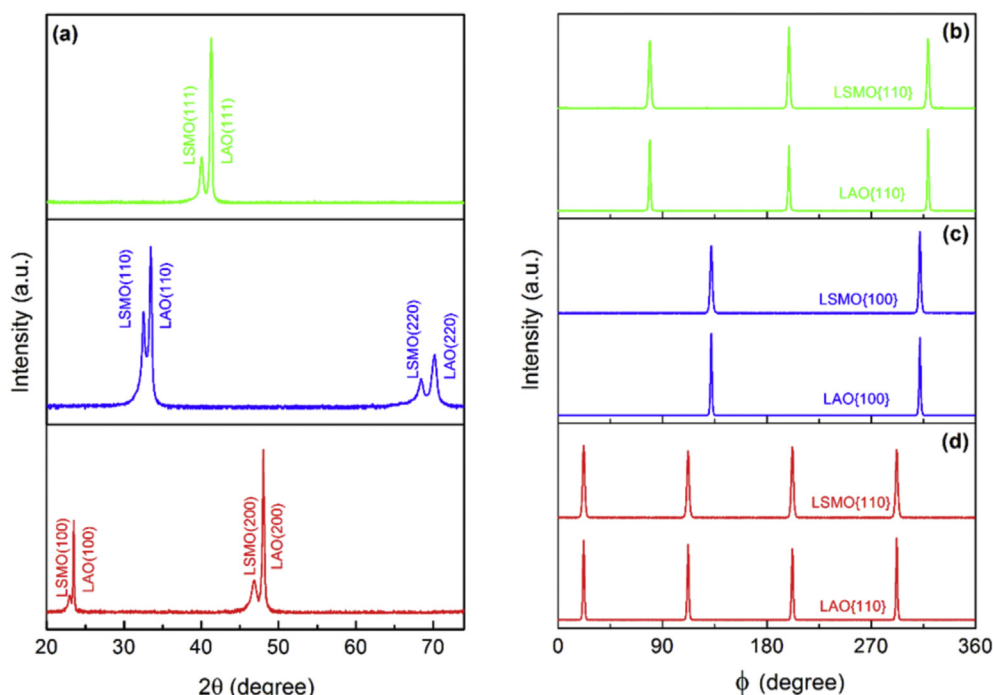


Fig. 1. (a) X-ray diffraction patterns of  $\theta$ - $2\theta$  scan for LSMO films on (100), (110), and (111) LAO substrates. X-ray  $\phi$ -scan for (b) LSMO (111), (c) LSMO (110), (d) LSMO (100).

Download English Version:

<https://daneshyari.com/en/article/5461396>

Download Persian Version:

<https://daneshyari.com/article/5461396>

[Daneshyari.com](https://daneshyari.com)